PCCP

Accepted Manuscript

ROYAL SOCIETY OF CHEMISTRY

www.rsc.org/pccp

Multi-responsive cellulose nanocrystal-rhodamine conjugates – An advanced structure study by solid-state dynamic nuclear polarization (DNP) NMR

Li Zhao,[a,1] Wei Li,[b] Andreas Plog,[c] Yeping Xu,[a] Gerd Buntkowsky,[a] Torsten Gutmann,[a]* Kai Zhang,[b,1]*

[a] *Eduard-Zintl-Institute for Inorganic Chemistry and Physical Chemistry, Technical University Darmstadt, Alarich-Weiss-Str. 4, D-64287 Darmstadt, Germany*
[b] *Ernst-Berl-Institute for Chemical Engineering and Macromolecular Science, Technical University Darmstadt, Alarich-Weiss-Str. 8, 64287 Darmstadt, Germany*
[c] *Center of Smart Interfaces, Technical University Darmstadt, Alarich-Weiss-Str.10, 64287 Darmstadt, Germany*

* Corresponding authors
K. Z.: zhang@cellulose.tu-darmstadt.de
T. G.: gutmann@chemie.tu-darmstadt.de

[1] These authors contribute equally to this work.

Abstract

Multi-stimuli responsive materials based on cellulose nanocrystals (CNC), especially using non-conventional stimuli including light, still need more explorations, to fulfill the requirement of complicated application environments. The structure determination of functional groups on CNC surface constitutes a significant challenge, partially due to their low amounts. In this study, rhodamine spiroamide groups are immobilized onto the surface of CNC leading to a hybrid compound being responsive to pH-value, heating and UV light. After the treatment with external stimuli, the fluorescent and correlated optical color change can be induced, which refers to a ring opening and closing process. Amine and amide groups in rhodamine spiroamide play the critical role during this switching process. Solid-state NMR spectroscopy coupled with sensitivity-enhanced dynamic nuclear polarization (DNP) was used to measure ^{13}C and ^{15}N in natural abundance, allowing the determination of structural changes during the switching process. It is shown that a temporary bond through an electrostatic interaction could be formed within the confined environment on the CNC surface during the heating treatment. The carboxyl groups on CNC surface plays a pivotal role in stabilizing the open status of rhodamine spiroamide groups.

Introduction

Crystalline nanocellulose in the form of cellulose nanocrystals (**CNC**) has attracted increasing interest in the last years.[1-5] It has been applied in various fields for the design of novel materials, e.g. as reinforcing material for high strength nano composites together with distinct polymers,[6, 7] for the formation of stimuli-responsive films,[8] hydrogels[9, 10] or light-healable materials,[11, 12] as template for the synthesis of chiral, nematic and porous materials, e.g. ethyl or acetyl/ethyl cellulose,[13] silica films[14] or TiO_2.[15] Moreover, **CNC** has been demonstrated to be biocompatible with living cells.[16, 17] Based on the non-cytotoxic property of **CNC**, it is an

excellent candidate for the preparation of biocompatible materials, such as for the bioimaging. Generally, the surface of **CNC** contains hydroxyl, carboxyl or sulfate groups depending on the synthesis procedure.[2, 16, 17] In particular, **CNC** with carboxyl groups on the surface, which can be obtained after the 2,2,6,6-tetramethylpiperidine-1-oxyl (TEMPO)-mediated oxidation of native cellulose fibers, shows the feasibility for the immobilization of further functional groups.[2, 16, 18]

Rhodamine, a popular fluorophore probe, has been investigated from the physical and chemical aspects owing to its excellent photo-physical properties and low cost.[19, 20] Depending on the external stimuli, rhodamine derivatives containing a spiroamide group enable a switching process between the fluorescent, open-ring amide and the non-fluorescent, close-ring spirolactam form. UV/heat-treatment and pH values are commonly used stimuli for switching the fluorescence and the correlated optical color of rhodamine derivatives. For such fluorophore sensors, the precise understanding of the structure-activity relationships is one of the most crucial steps to develop new materials with advanced functions.[21] The synthesis of hybrid compounds with switchable rhodamine spiroamide groups immobilized on the surface of **CNC** which still maintains the stimuli-responsive properties of rhodamine spiroamide has not been realized up to now. In addition to the synthesis of the **CNC**-rhodamine spiroamide, it is hitherto still unknown how the chemical structures of responsive functional groups are affected during their dynamic switching process in a confined environment on the **CNC** surface.

Solution NMR techniques were generally used to study rhodamine derivatives. However, solution NMR shows limitations for hybrid materials, which cannot be dissolved by common solvents. In contrast, solid-state NMR (ssNMR) spectroscopy is a powerful technique for characterizing such hybrid materials, providing the potential of investigating the structure of grafted molecules.[22-30] Nevertheless, the low sensitivity of ssNMR restricts the detection of surface species, especially for target nuclei containing low gamma and/or quadrupolar moment (e.g. ^{13}C, ^{15}N, ^{17}O, etc.) in natural abundance.[31] Techniques such as cross polarization (CP) transfer from protons to less sensitive hetero nuclei increase the sensitivity.[32] However, long measurement times from several hours to days are often still required to get a reasonable signal-to-noise (S/N) ratio. A promising method to increase the NMR sensitivity in solid systems is the so-called hyperpolarization, which employs the larger polarization of rotational energy levels (i.e. PHIP),[33-35] or of electron spins (i.e. SEOP).[36, 37] A further very powerful method is dynamic nuclear polarization (DNP), which utilizes the polarization of unpaired electrons from stable radicals or paramagnetic species and transfer them into nuclear spin polarization.[38-41] Although this technique was originally developed for low magnetic fields, DNP made significant progress in high field ssNMR in the past years, when gyrotron systems became applicable as microwave source.[42-45] Very recently, a number of works demonstrating the successful use of DNP in the field of surface chemistry have been reported,[46-51] which also includes the studies on cellulose samples.[52-54] As a prominent example, Wang et al.[55] applied DNP to investigate the binding target of the tiny amount protein fragment involved in cell growth.

Inspired by these previous works, we used DNP to investigate the novel, multi-stimuli responsive cellulose nanocrystals (**CNC**) with surface-doped rhodamine derivatives, to shed more light on the color switching process of this compound from the structural point of view. In the first section, the synthesis and basic characterization of **CNC** with surface-immobilized rhodamie spiroamide groups (**CNC-RhB**) is described. In the next step, the stimuli-responsive behavior and the tunable fluorescence of **CNC-RhB** with respect to diverse stimuli were investigated, which includes pH values, UV-illumination and heat treatment. Finally, the modified chemical structures of rhodamine spiroamide during the switching process in its constrained status were analyzed, employing solid-state ^{13}C and ^{15}N CP MAS NMR spectroscopy combined with dynamic nuclear polarization (DNP) to enhance the sensitivity.

The spectra show excellent S/N ratios and sufficient resolution to observe the stimuli-induced structure change of rhodamine spiroamide groups immobilized on the **CNC** surface.

Results and discussion

Synthesis of CNC and CNC-RhB

Cellulose nanocrystals (**CNC**) with diameters of around 5 nm (Figure 1a) were obtained after the TEMPO-mediated oxidation of microcrystalline cellulose.[18, 56] According to the conductive titration, the surface of **CNC** is decorated with carboxyl groups as well as carbonyl groups of 1.102 mmol/g and 0.053 mmol/g, respectively (Figure S1).[57] In the second step, rhodamine spiroamide groups were immobilized on the surface of **CNC** after reaction between carboxyl groups and the amino groups of aminoethyl rhodamine (Figure 1b & Figure S2), leading to **CNC** with surface-attached rhodamine (**CNC-RhB**). The amount of immobilized aminoethyl rhodamine was determined to be 0.2±0.01 mmol/g based on the elemental analysis. The obtained product is well dispersible in DMF and still maintains its diameter between 5-6 nm as evidenced by AFM (Figure 1c). The introduction of rhodamine on the **CNC** surface was confirmed by FTIR (Figure S3). Next to the FTIR bands assigned to carboxyl groups at 1609 cm^{-1}, **CNC-RhB** exhibits new bands at 1720 and 1655 cm^{-1} referring vibrations of amide groups.[58]

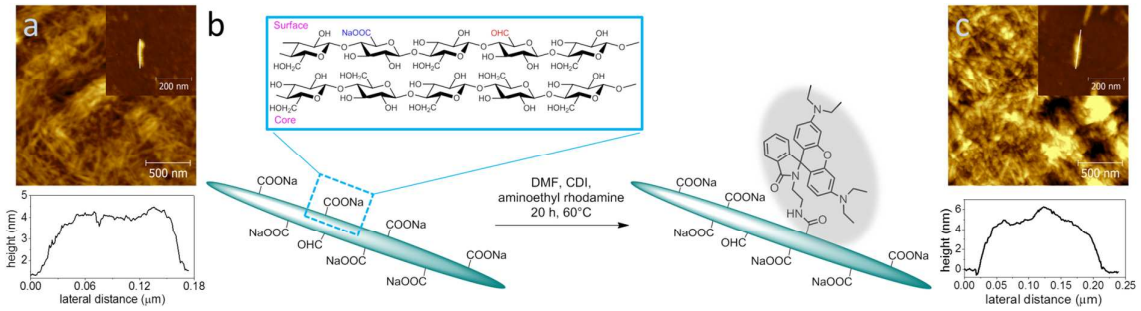

Figure 1. (a) AFM image of cellulose nanocrystals (**CNC**) prepared by TEMPO-mediated oxidation of microcrystalline cellulose. (b) Schematic representation of the modification of the **CNC** surface by aminoethyl rhodamine. (c) AFM image of **CNC** with surface-attached aminoethyl rhodamine (**CNC-RhB**).

Switching properties of CNC-RhB

After the synthesis, **CNC-RhB** in DMF at neutral pH-value shows beige color (Figure 2a & Figure S4). By applying external stimuli, such as UV-illumination/heat-treatment or alteration of the pH value, the optical color of the corresponding fluorescence of **CNC-RhB** changes as illustrated in Figure S4. Switching the optical color of **CNC-RhB** based on pH values is not surprising since the color depends on the chemical structure of the rhodamine spiroamide which changes in response to the pH value (Figure S4a).[59, 60] By adding acid, such as aqueous HCl solution, the color became magenta, while the addition of aqueous NaOH solution led to beige color again. Moreover, if the solvent was changed from DMF into water, the color of **CNC-RhB** switched to magenta due to the polar environment and thus the presence of the assumed open-ring spiroamide (Figure S4b). Although the reaction condition during the amide formation and following washing process allowed the carboxyl groups to stay in its salt-form with sodium cations, they could interact with water and release protons after

sufficient time (Figure S4c). Subsequently, the rings of rhodamine spiroamide are opened and the compound color turned to magenta. The removal of water from the system under vacuum led to beige **CNC-RhB** again. After replacement of DMF by water, **CNC-RhB** suspended in water also exhibited the switchable feasibility in response to pH values (Figure S4d). By adding aqueous HCl or NaOH solution, the color of the suspension can be reversibly switched between magenta and beige color.

In addition to the pH value, the color of **CNC-RhB** suspended in DMF also switches by UV-illumination and heat-treatment (Figure 2a). UV-illumination at 365 nm for 10 min turned its beige color to magenta, while heat-treatment at 130°C for 10 min led to the disappearance of the magenta color. In accordance with the optical color change, the fluorescence intensity of the suspensions is strong for the magenta suspension and weak for the beige suspension, according to the characteristic signal group at 587 nm for rhodamine (Figure 2b). It is also notable that the fluorescence intensity could not be totally recovered after UV-illumination for the same time. After two cycles, the fluorescence decreased to ~75% of the original fluorescence. Especially, the heat-treatment significantly lowered the fluorescence of **CNC-RhB**, as shown by the low fluorescence intensity after 1 h heat treatment and subsequent 10 min UV-illumination, resulting in **CNC-RhB** with only ~45% of the original fluorescence.

The switching of the optical color and the correlated fluorescence of pristine rhodamine spiroamide molecules or rhodamine spiroamide at polymer chains is derived from the structural change between closed (weakly fluorescent) and open form (strongly fluorescent) in response to pH values, UV-illumination and heating.[60, 61] Thus, the rhodamine molecules at CNC surface should undergo similar switching processes (Figure 2d).

Furthermore, heat-treatment for 1 h at 130°C of **CNC-RhB** suspended in DMF with neutral pH value resulted in **CNC-RhB-130°C** with an optically brown color of the suspension (Figure S4e). After further UV-illumination at 365 nm for 10 min, the color became peach-puff instead of magenta, and subsequent heat-treatment led to brown color again. The treatment can be repeated with color reversibility depending on the external stimuli. The detailed fluorescence spectroscopic analysis on the as-treated **CNC-RhB** suspensions in DMF showed the characteristic bands for rhodamine at 586 nm (Figure 2e). Moreover, the signal intensity of **CNC-RhB-130°C** after the first UV-treatment is only 84±4% of that of **CNC-RhB** in DMF after the first UV-treatment (normalized to 100%, Figure 2c and 2f). The addition of aqueous NaOH solution (5 wt.%) turns the brown color of the **CNC-RhB** suspension back to beige color. Hence, there should be a temporary binding between carboxyl groups and rhodamine spiroamide, which can be restored by aqueous NaOH solution. Probably, the heat-treatment resulted in cross-linking, e.g. a temporary amide groups between carboxyl groups and rhodamine spiroamide on the surface of **CNC**, which could stabilize the open ring structure. At the same time, the formation of these new cross-linking bonds was accompanied by the appearance of the optically brown color. The cross-linkers could be reversely cleaved by the alkaline treatment and restored by heat-treatment. Thus, the rhodamine backbone still maintained during the reversible treatments, which still shows characteristic fluorescence signal.

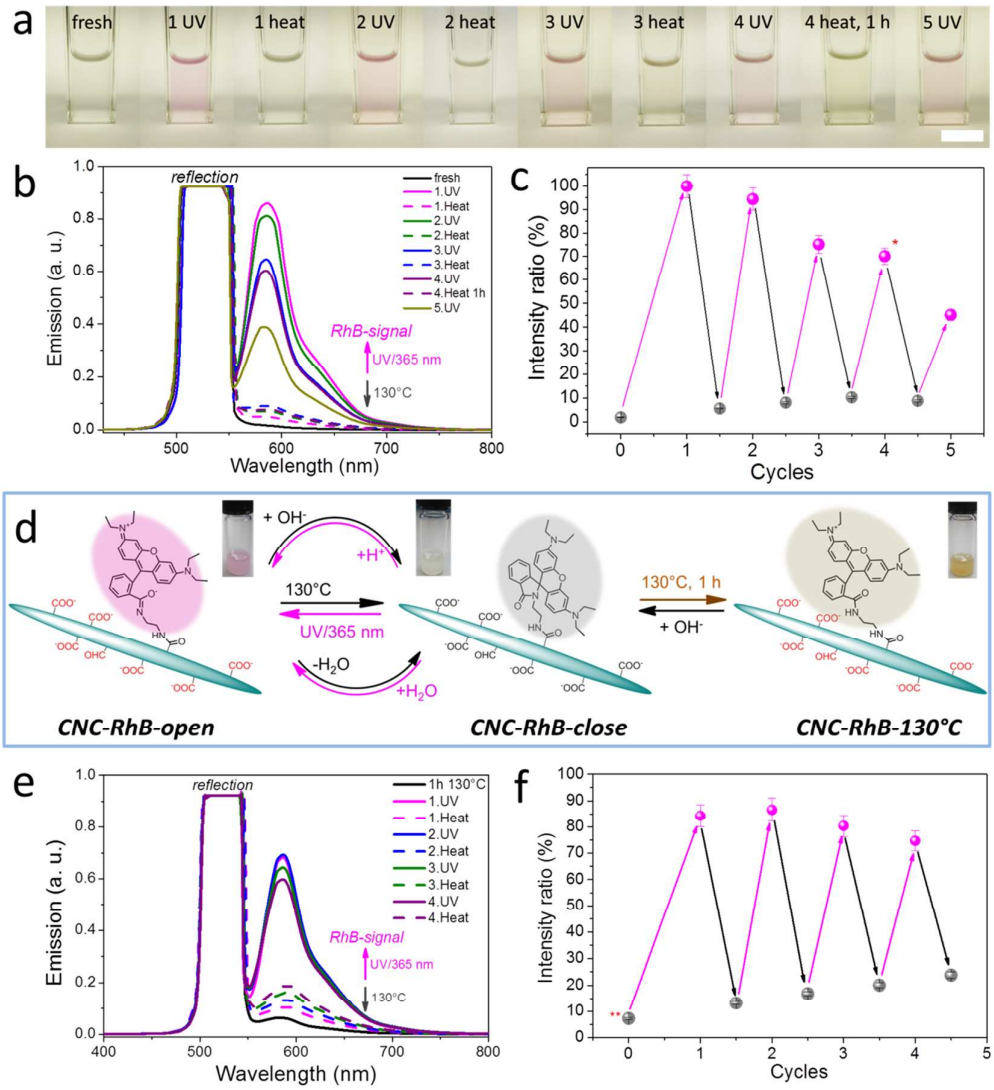

Figure 2. Multi-responsive behavior of **CNC-RhB** suspended in DMF. (a) Pictures of the **CNC-RhB**/DMF suspensions after UV-illumination at 365 nm and heat treatment at 130°C for 5 cycles. (b) Corresponding fluorescence spectra of the suspensions in (a). (c) Plot of the intensity ratios of the signals around 590 nm. *Note:* The signal intensity after the first UV treatment was set as 100%. * The 4th heat-treatment was 1 h. (d) Schematic illustration of the switching behavior of **CNC-RhB** in DMF (8.9 mg/ml). (e) Fluorescence spectra of **CNC-RhB** suspended in DMF after 1 h heat-treatment at 130°C, UV-illumination for 10 min as well as following repeated cycles. (f) Plot of the intensity ratios of the signals at 587 nm with the signal intensity of **CNC-RhB** in DMF after the first UV-illumination in Figure 2c set as 100%. ** The starting suspension of **CNC-RhB** in DMF was treated at 130°C for 1 h.

Solid-state ^{13}C and ^{15}N DNP NMR spectroscopy

CNC contains both carboxyl groups (together with a low amount of aldehyde groups) and hydroxyl groups at its surface.[1, 2] However, only few sites are covered with rhodamine spiroamide (appr. 0.2±0.01 mmol/g), which hampers the detection of this functionality with standard NMR techniques. As a consequence, the low sensitivity makes the analysis of induced structural changes of the rhodamine spiroamide moieties difficult. Thus, solid-state

^{13}C and ^{15}N NMR spectroscopy combined with DNP enhancement was employed, in order to detect these structural changes including carbonyl, amide as well as the methylene groups. The DNP measurements required a special sample preparation including a solvent matrix containing the stable radical AMUpol. This radical matrix is used as both polarization source and polarization transfer medium. To exclude the effect of the matrix containing the AMUPol radical on the structural changes of the **CNC-RhB**, ^{13}C NMR spectra with and without radical matrix were performed. These spectra illustrate that the presence of the matrix at low temperature did not cause significant change of the line shape and thus structural modification (Figure S7).

In the first step, ^{13}C CP MAS measurements with mw irradiation were performed for **CNC** and **CNC-RhB** at equal conditions (Figure 3a). Comparing the spectra before and after doping, it is visible that the signals attributed to the carbons (C1-6) in the anhydroglucose units (AGUs) of the cellulose are not significantly affected, while new signals for carbonyl carbons in the region of 165 to 190 ppm (Figure 3b), and for aliphatic carbons in the region from 0 to 50 ppm (Figure 3c) appeared. This clearly shows that the rhodamine derivative was successfully bound on the surface of **CNC**.

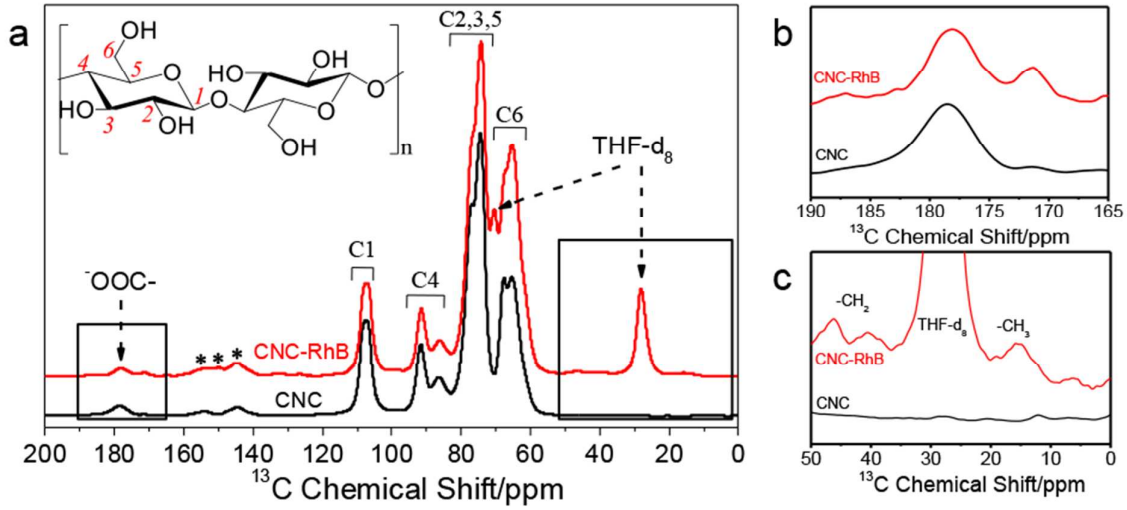

Figure 3. (a) ^{13}C CP MAS spectra with mw irradiation of **CNC** and **CNC-RhB** after alkaline treatment. The inset in (a) shows the representative numbering of carbon atoms (1-6) within the anhydroglucose units (AGUs) of cellulose. Both NMR spectra in (a) were recorded with 64 scans. *Note:* Signals marked with * are spinning sidebands. (b) Enlarged spectrum of the carbonyl carbons (from 165 to 190 ppm). (c) Enlarged spectrum of the alkyl carbon (from 0 to 50 ppm).

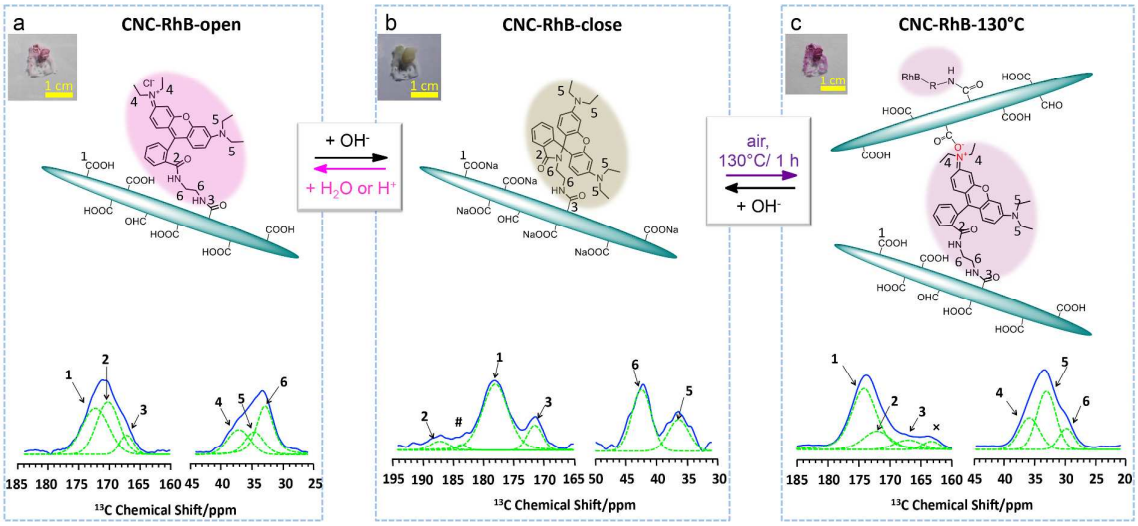

Figure 4. Schematic illustration for the switching behavior of the dried **CNC-RhB** samples. The enlarged solid-state ^{13}C NMR spectra of (a) **CNC-RhB-open**, (b) **CNC-RhB-close** and (c) **CNC-RhB-130°C** and the deconvoluted signals of the carbonyl region (from 160 to 195 ppm) and the region of methylene groups (from 20 to 50 ppm). *Note:* Small signals marked with # caused by base line fluctuation and × refer to aldehyde groups.

CNC-RhB-close in the closed-ring form was transferred from its DMF-suspension into acetone showed beige color (Figure 4b). During drying under air at RT, the color slowly changed to magenta after the adsorption of water. During this process, the carboxyl groups and the ring amide were protonated, leading to **CNC-RhB-open** with rhodamine spiroamide as open-ring form (Figure 4a). Heat-treatment of the **CNC-RhB-close** at 130°C for 1 h yielded dried **CNC-RhB-130°C** with intensive purple color (Figure 4c), for which also an open ring structure is assumed. These two expected open-ring forms can be switched back to beige **CNC-RhB-close**, by adding aqueous NaOH solution as displayed by the color change from magenta or purple to beige. Thus, in the next step, all three proposed forms **CNC-RhB-open**, **CNC-RhB-close** and **CNC-RhB-130°C** were analyzed in detail employing ^{13}C CP MAS NMR with mw irradiation. The ^{13}C enhancement factors as indication for the improvement of the S/N ratio were calculated as 28, 30 and 41 for **CNC-RhB-open**, **CNC-RhB-close** and **CNC-RhB-130 °C**, respectively (Figure S8).

Details of the ^{13}C CP MAS spectra are shown in Figure 4. Signals were deconvoluted according to ref.[62] Thus, the carbonyl region (160 to 195 ppm) was deconvoluted into three signals that are assigned to free carboxyl groups on the **CNC** surface (**CNC**-COOH) (**1**), spiroamide groups or phenyl amide groups within spirolactam groups (Ph-CO-NH) (**2**) and amide carbons referring rhodamine spiroamide attached to **CNC** (-HNCO-**CNC**) (**3**). The region of methylene groups (20 to 50 ppm) were deconvoluted into several signals for -$H^+N(CH_2CH_3)_2$ groups (**4**), -$N(CH_2CH_3)_2$ groups (**5**) and -$HNCH_2CH_2NH$- moieties (**6**), respectively.

The ^{13}C NMR signals for carboxyl groups on the **CNC** surface (**1**) range from 173 to 178 ppm depending on the chemical environment. Carboxyl groups present in the sodium salt form yield a ^{13}C chemical shift to lower fields (larger ppm values) compared to the COOH group. After binding of rhodamine molecules via an amide bond (**3**), the ^{13}C chemical shift of carboxyl function on the **CNC** surface changed to higher fields (lower ppm values) by approximately 6 ppm. The significantly different color between **CNC-RhB-close** and **CNC-RhB-open** is related to the status of the spirolactam and the amide functionality within the rhodamine moieties. Accordingly, the ^{13}C chemical shift at 187 ppm assigns the spiro-carbon

in **CNC-RhB-close** (187 ppm) (Figure 4b, **2**) while the signals around 170 to 173 ppm refer to the amide carbon in **CNC-RhB-open** (Figure 4a and 4c, **2**). In the aliphatic region of **CNC-RhB-close,** two signals at 36 and 43 ppm are distinguishable referring to -N($\underline{C}H_2CH_3)_2$ groups (**5**) and -NH$\underline{C}H_2\underline{C}H_2$NH- moieties (**6**), respectively. Another result is found for the **CNC-RhB-open** and **CNC-RhB-130°C** systems, where a third signal appeared at around 36 ppm due to the protonation of the –NEt_2 groups forming –HN($\underline{C}H_2CH_3)_2^+$ (**4**).

The ^{15}N CP MAS spectra of **CNC-RhB-open**, **CNC-RhB-close** and **CNC-RhB-130°C** display characteristic signals attributed to nitrogen species of rhodamine groups (Figure 5), which directly provides structural information of the amide/spirolactam group. A signal at –261 ppm (**II**) is observed for all three samples, which is ascribed to the amide group formed during immobilization of the rhodamine molecules. When monitoring the reaction from **CNC-RhB-close** to **CNC-RhB-open** employing ^{15}N CP MAS (Figure 5a & 5b), only slight change of the NMR spectrum is observed. The ^{15}N NMR signal at –223 ppm (**I**) indicates that rhodamine moieties with spiro-carbon are also present in the **CNC-RhB-open** sample. Even with excess of HCl the spiro form prevailing in its equilibrium. Interestingly, the ^{13}C NMR signal around 187 ppm for the spiro-carbon in **CNC-RhB-open** shows no significant intensity. This observation might refer to the hydrophobicity of the spiro groups, which reduce the polarization efficiency with a hydrophilic matrix.

The peak at –301 ppm (**III**) observed in all three systems represents -$\underline{N}Et_2$ groups within RhB. A 11-ppm low-field shifted signal at –290 ppm (**IV**) is only visible for **CNC-RhB-close** (Figure 5b), which is a clear hint that hydrogen bonds of the -$\underline{N}Et_2$ with surrounding water are built up (Figure 5b').[63, 64] The resonance at –308 ppm (**V**) seems to be related to -H$\underline{N}Et_2^+$ groups, which are formed after adding HCl (Figure 5a').[65, 66]

The ^{15}N NMR spectrum of **CNC-RhB-130°C** shows the disappearance of the spirolactam signal at –223 ppm (**I**) and the appearance of a new signal at –205 ppm (**VI**) corresponding to amide groups. In addition, **CNC-RhB-130°C** displays a second new signal at –355 ppm (**VII**).

The intensity of this signal is similar to that of the signal at –308 ppm in the NMR spectrum of **CNC-RhB-open**. Therefore, we assume that the signal at –355 ppm originates from the protonated nitrogen (-HNEt_2^+) that interacts with the residual carboxylate anion (-COO^-) on the other **CNC** surface formed during heating (Figure 5c'). This cross-linking should be contributed to the static electronic force, because **CNC-RhB-130°C** could be switched back to **CNC-RhB-close** after the treatment with NaOH and they show an excellent switching performance. This will also explain why the rhodamine-derived compound changed its color from magenta into purple during heat-treatment and not into beige or white as expected from the literature.[59]

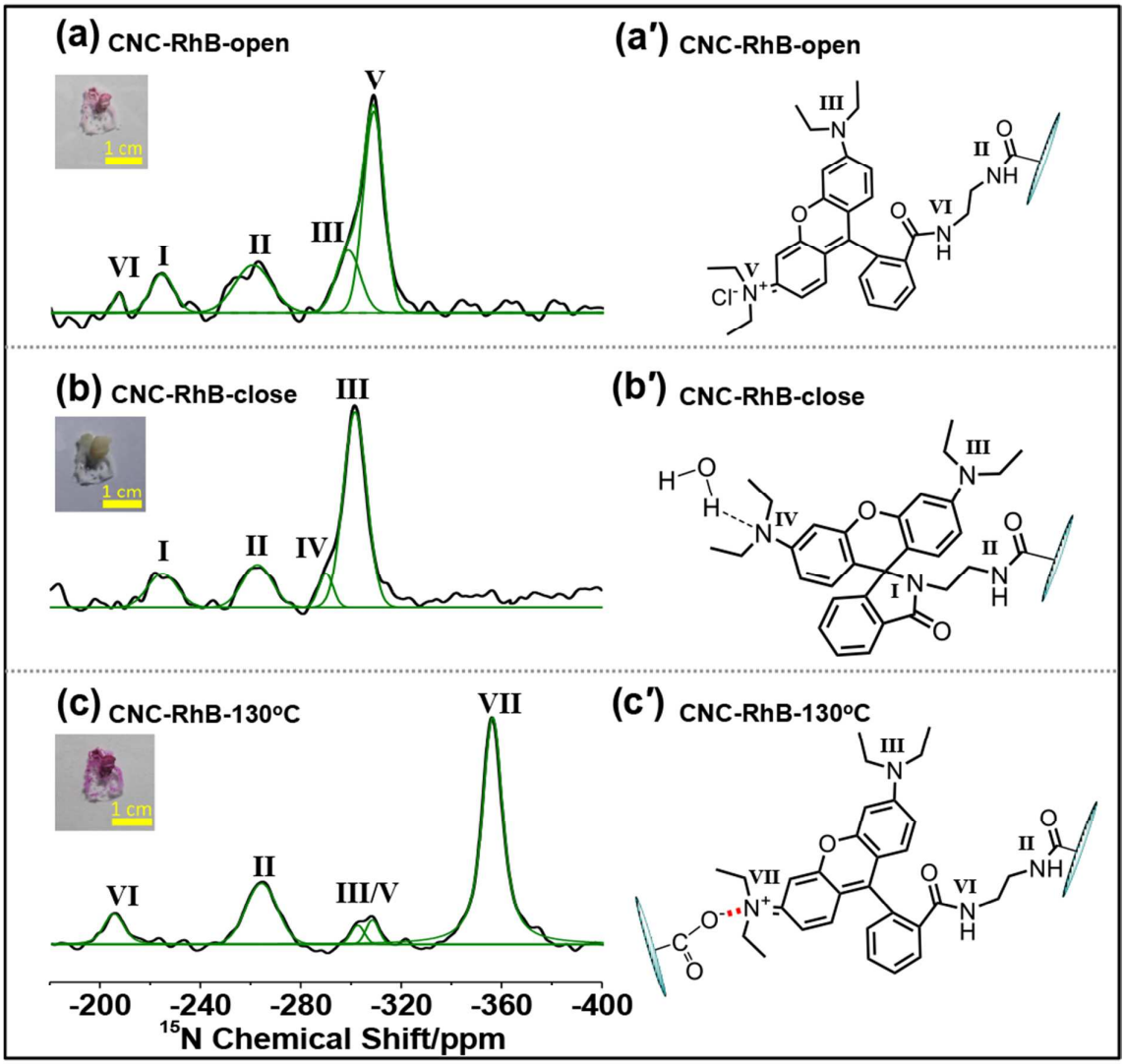

Figure 5. Solid-state DNP-enhanced ^{15}N NMR spectra of **CNC-RhB** samples (a-b) and schematic representation of their chemical structures (a'-c'): **CNC-RhB-open** (a, a'), **CNC-RhB-close** (b, b'), and **CNC-RhB-130°C** (c, c'). The sizes of the CNC and the rhodamine molecules are not in the real scale.

Conclusion

We show for the first time the synthesis of multi-stimuli responsive materials based on cellulose nanocrystals (**CNC**) after the immobilization of rhodamine spiroamide at **CNC** surface. The optical color and fluorescence of the conjugate can not only be switched in response to pH values, but also UV-illumination and heating. Furthermore, the solid-state ^{13}C/^{15}N DNP NMR spectroscopy was successfully applied to analyze the chemical environment at **CNC** surface. The structural change of rhodamine spiroamide immobilized on **CNC** surface could be explicitly detected, in spite of its amount of 0.2±0.01 mmol/g. In particular, the amine and amide groups in **CNC-RhB** conjugates could be detected using solid-state ^{13}C/^{15}N DNP NMR, in order to illustrate the structural change during the switching process: **CNC-RhB-close** containing close-ring spiroamide and **CNC-RhB-open** containing open-ring spirolactam. Moreover, another structural form of **CNC-RhB** conjugates after the heat-treatment at 130°C was revealed (**CNC-RhB-130°C**), which was stabilized through an

electrostatic interaction. The confined environment at **CNC** surface with the presence of carboxyl groups played a pivotal role in stabilizing the structure. Based on the advantages of **CNC**, such as the biocompatibility, non-cytotoxicity and abundance of cellulose in nature, smart and multi-functional compounds using **CNC** are promising candidates for wide applications.

Acknowledgements
This work has been supported by the Deutsche Forschungsgemeinschaft (DFG) under contract Bu-911-20-1 that gave us the opportunity to set-up the DNP spectrometer. The authors thank the Hessian excellence initiative LOEWE – research cluster SOFT CONTROL (Hessen, Germany) for financial support. A. Geissler is acknowledged for the fluorescence spectroscopic measurements. W.L. thanks the Chinese Scholarship Council (CSC) for the financial support.

Notes and references

1. R. J. Moon, A. Martini, J. Nairn, J. Simonsen and J. Youngblood, *Chem. Soc. Rev.*, 2011, **40**, 3941-3994.
2. Y. Habibi, L. A. Lucia and O. J. Rojas, *Chem. Rev.*, 2010, **110**, 3479-3500.
3. D. Klemm, F. Kramer, S. Moritz, T. Lindstrom, M. Ankerfors, D. Gray and A. Dorris, *Angew. Chem. Int. Ed.*, 2011, **50**, 5438-5466.
4. Y. Habibi, *Chem. Soc. Rev.*, 2014, **43**, 1519-1542.
5. P. Tingaut, T. Zimmermann and G. Sebe, *J. Mater. Chem.*, 2012, **22**, 20105-20111.
6. J. R. Capadona, O. Van Den Berg, L. A. Capadona, M. Schroeter, S. J. Rowan, D. J. Tyler and C. Weder, *Nat. Nanotechnol.*, 2007, **2**, 765-769.
7. J. R. Capadona, K. Shanmuganathan, D. J. Tyler, S. J. Rowan and C. Weder, *Science*, 2008, **319**, 1370-1374.
8. J. D. Fox, J. R. Capadona, P. D. Marasco and S. J. Rowan, *J. Am. Chem. Soc.*, 2013, **135**, 5167-5174.
9. J. A. Kelly, A. M. Shukaliak, C. C. Cheung, K. E. Shopsowitz, W. Y. Hamad and M. J. MacLachlan, *Angew. Chem. Int. Ed.*, 2013, **52**, 8912-8916.
10. J. R. Mckee, S. Hietala, J. Seitsonen, J. Laine, E. Kontturi and O. Ikkala, *Acs Macro Lett.*, 2014, **3**, 266-270.
11. M. V. Biyani, E. J. Foster and C. Weder, *Acs Macro Lett.*, 2013, **2**, 236-240.
12. S. Coulibaly, A. Roulin, S. Balog, M. V. Biyani, E. J. Foster, S. J. Rowan, G. L. Fiore and C. Weder, *Macromolecules*, 2014, **47**, 152-160.
13. S. Shimamoto and D. G. Gray, *Chem. Mater.*, 1998, **10**, 1720-1726.
14. K. E. Shopsowitz, H. Qi, W. Y. Hamad and M. J. Maclachlan, *Nature*, 2010, **468**, 422-425.
15. K. E. Shopsowitz, A. Stahl, W. Y. Hamad and M. J. MacLachlan, *Angew. Chem. Int. Ed.*, 2012, **51**, 6886-6890.
16. K. A. Mahmoud, J. A. Mena, K. B. Male, S. Hrapovic, A. Kamen and J. H. Luong, *ACS Appl. Mater. Interfaces*, 2010, **2**, 2924-2932.
17. S. Dong, H. J. Cho, Y. W. Lee and M. Roman, *Biomacromolecules*, 2014, **15**, 1560-1567.
18. T. Saito and A. Isogai, *Biomacromolecules*, 2004, **5**, 1983-1989.
19. R. Ramette and E. Sandell, *J. Am.Chem. Soc.*, 1956, **78**, 4872-4878.
20. B. Valeur and M. N. Berberan-Santos, *Molecular fluorescence: principles and applications*, John Wiley & Sons, 2013.
21. H. N. Kim, M. H. Lee, H. J. Kim, J. S. Kim and J. Yoon, *Chem. Soc. Rev.*, 2008, **37**, 1465-1472.
22. S. M. De Paul, J. W. Zwanziger, R. Ulrich, U. Wiesner and H. W. Spiess, *J. Am. Chem. Soc.*, 1999, **121**, 5727-5736.
23. M. Templin, U. Wiesner and H. W. Spiesss, *Adv. Mater.*, 1997, **9**, 814-817.
24. L. Zhao, Z. Qi, F. Blanc, G. Yu, M. Wang, N. Xue, X. Ke, X. Guo, W. Ding, C. P. Grey and L. Peng, *Adv. Funct. Mater.*, 2014, **24**, 1696-1702.
25. S. Abdulhussain, H. Breitzke, T. Ratajczyk, A. Gruenberg, M. Srour, D. Arnaut, H. Weidler, U. Kunz, H. J. Kleebe, U. Bommerich, J. Bernarding, T. Gutmann and G. Buntkowsky, *Chem. - Eur. J.*, 2014, **20**, 1159-1166.
26. J. Bluemel, *Coord. Chem. Rev.*, 2008, **252**, 2410-2423.
27. A. Grünberg, H. Breitzke and G. Buntkowsky, *Spectroscopic Properties of Inorganic and Organometallic Compounds: Techniques, Materials and Applications*, 2012, **43**, 289-323.
28. T. Gutmann, A. Gruenberg, N. Rothermel, M. Werner, M. Srour, S. Abdulhussain, S. Tan, Y. Xu, H. Breitzke

and G. Buntkowsky, *Solid State Nucl. Magn. Reson.*, 2013, **55-56**, 1-11.
29. J. Trebosc, J. W. Wiench, S. Huh, V. S. Y. Lin and M. Pruski, *J. Am. Chem. Soc.*, 2005, **127**, 7587-7593.
30. K. Mao, T. Kobayashi, J. W. Wiench, H.-T. Chen, C.-H. Tsai, V. S. Y. Lin and M. Pruski, *J. Am. Chem. Soc.*, 2010, **132**, 12452-12457.
31. C. Fernandez and M. Pruski, in *Solid State NMR*, ed. J. C. C. Chan, Springer Berlin Heidelberg, 2012, **141**, 119-188.
32. M. J. Duer, *Solid state NMR spectroscopy: principles and applications*, John Wiley & Sons, 2008.
33. S. S. Arzumanov and A. G. Stepanov, *J. Phys. Chem. C*, 2013, **117**, 2888-2892.
34. H. Henning, M. Dyballa, M. Scheibe, E. Klemm and M. Hunger, *Chem. Phys. Lett.*, 2013, **555**, 258-262.
35. A. A. Lysova and I. V. Koptyug, *Chem. Soc. Rev.*, 2010, **39**, 4585-4601.
36. W. Happer, E. Miron, S. Schaefer, D. Schreiber, W. A. van Wijngaarden and X. Zeng, *Phys. Rev. A*, 1984, **29**, 3092-3110.
37. J. L. Bonardet, J. Fraissard, A. Gedeon and M. A. Springuel-Huet, *Catal. Rev.*, 1999, **41**, 115-225.
38. T. Carver and C. Slichter, *Phys. Rev.*, 1953, **92**, 212.
39. A. W. Overhauser, *Phys. Rev.*, 1953, **92**, 411.
40. U. Akbey, B. Altin, A. Linden, S. Ozcelik, M. Gradzielski and H. Oschkinat, *Phys. Chem. Chem. Phys.*, 2013, **15**, 20706-20716.
41. D. Lee, H. Takahashi, A. S. L. Thankamony, J.-P. Dacquin, M. Bardet, O. Lafon and G. D. Paëpe, *J. Am. Chem. Soc.*, 2012, **134**, 18491-18494.
42. K. R. Thurber, W.-M. Yau and R. Tycko, *J. Magn. Reson.*, 2010, **204**, 303-313.
43. R. Griffin and T. Prisner, *Phys. Chem. Chem. Phys.*, 2010, **12**, 5737-5740.
44. S. Reynolds and H. Patel, *Appl. Magn. Reson.*, 2008, **34**, 495-508.
45. V. Vitzthum, M. A. Caporini and G. Bodenhausen, *J. Magn. Reson.*, 2010, **205**, 177-179.
46. A. Lesage, M. Lelli, D. Gajan, M. A. Caporini, V. Vitzthum, P. Miéville, J. Alauzun, A. Roussey, C. Thieuleux, A. Mehdi, G. Bodenhausen, C. Coperet and L. Emsley, *J. Am. Chem. Soc.*, 2010, **132**, 15459-15461.
47. A. J. Rossini, A. Zagdoun, M. Lelli, A. Lesage, C. Copéret and L. Emsley, *Acc. Chem. Res.*, 2013, **46**, 1942-1951.
48. F. Pourpoint, A. S. L. Thankamony, C. Volkringer, T. Loiseau, J. Trebosc, F. Aussenac, D. Carnevale, G. Bodenhausen, H. Vezin, O. Lafon and J.-P. Amoureux, *Chem. Commun.*, 2014, **50**, 933-935.
49. O. Lafon, A. S. L. Thankamony, T. Kobayashi, D. Carnevale, V. Vitzthum, I. I. Slowing, K. Kandel, H. Vezin, J.-P. Amoureux, G. Bodenhausen and M. Pruski, *J. Phys. Chem. C*, 2012, **117**, 1375-1382.
50. T. Kobayashi, O. Lafon, A. S. Lilly Thankamony, I. I. Slowing, K. Kandel, D. Carnevale, V. Vitzthum, H. Vezin, J.-P. Amoureux, G. Bodenhausen and M. Pruski, *Phys. Chem. Chem. Phys.*, 2013, **15**, 5553-5562.
51. D. Lee, G. Monin, N. T. Duong, I. Z. Lopez, M. Bardet, V. Mareau, L. Gonon and G. De Paëpe, *J. Am. Chem. Soc.*, 2014, **136**, 13781-13788.
52. H. Takahashi, I. Ayala, M. Bardet, G. l. De Paëpe, J.-P. Simorre and S. Hediger, *J. Am. Chem. Soc.*, 2013, **135**, 5105-5110.
53. H. Takahashi, D. Lee, L. Dubois, M. Bardet, S. Hediger and G. De Paëpe, *Angew. Chem.*, 2012, **124**, 11936-11939.
54. R. A. Wind, L. Li, G. E. Maciel and J. B. Wooten, *Appl. Magn. Reson.*, 1993, **5**, 161-176.
55. T. Wang, Y. B. Park, M. A. Caporini, M. Rosay, L. Zhong, D. J. Cosgrove and M. Hong, *Proc. Natl. Acad. Sci.*, 2013.
56. T. Saito, S. Kimura, Y. Nishiyama and A. Isogai, *Biomacromolecules*, 2007, **8**, 2485-2491.
57. K. Zhang, S. Fischer, A. Geissler and E. Brendler, *Carbohydr. Polym.*, 2012, **87**, 894-900.
58. G. Socrates, *Infrared and Raman characteristic group frequencies*, Wiley, England, 2001.
59. C. G. Schäfer, M. Gallei, J. T. Zahn, J. Engelhardt, G. P. Hellmann and M. Rehahn, *Chem. Mater.*, 2013, **25**, 2309-2318.
60. Y. Shiraishi, R. Miyamoto, X. Zhang and T. Hirai, *Org. Lett.*, 2007, **9**, 3921-3924.
61. M. Beija, C. A. Afonso and J. M. Martinho, *Chem. Soc. rev.*, 2009, **38**, 2410-2433.
62. J.-S. Wu, I.-C. Hwang, K. S. Kim and J. S. Kim, *Org. Lett.*, 2007, **9**, 907-910.
63. B. Kamieński, W. Schilf, T. Dziembowska, Z. Rozwadowski and A. Szady-Chełmieniecka, *Solid State Nucl. Magn. Reson.*, 2000, **16**, 285-289.
64. S. Sharif, M. C. Huot, P. M. Tolstoy, M. D. Toney, K. H. M. Jonsson and H.-H. Limbach, *J. Phys. Chem. B*, 2007, **111**, 3869-3876.
65. A. Dos, V. Schimming, S. Tosoni and H.-H. Limbach, *J. Phys. Chem. B*, 2008, **112**, 15604-15615.
66. A. Dos, V. Schimming, M. Chan-Huot and H.-H. Limbach, *Phys. Chem. Chem. Phys.*, 2010, **12**, 10235-10245.